Surgical and Radiologic Anatomy (2019) 41:801–808
https://doi.org/10.1007/s00276-019-02220-z

ORIGINAL ARTICLE

New detailed description of the anterior part of the cribriform plate using anatomic specimens and computed tomography

Clément Escalard[1] · Lise-Marie Roussel[2] · Michèle Hamon[1] · Apolline Kazemi[3] · Vincent Patron[2] · Martin Hitier[2,4,5]

Received: 20 December 2018 / Accepted: 11 March 2019 / Published online: 21 March 2019

Abstract

Purpose Ethmoidal slit (ES) and cribroethmoidal foramen (CF) have been poorly studied, without any radiological description. They may ease cribriform plate's diseases. The objective was to describe the frequency, size, and computed tomography (CT) appearance of these foramina.

Methods A two-part anatomoradiological study was performed: first on dry skulls using a surgical microscope and CT, second on patients CT scans. For each, foramina were searched for, described, and measured when possible.

Results Thirteen dry macerated skulls were studied. The orbitomeatal plane was relevant for studying ES. With microscope, ES and CF were identified in, respectively, 92% and 100% of cases. Using CT, all ES and CF were visible, with a mean length and width of, respectively, 3.9 ± 1.7 mm and 0.9 ± 0.3 mm for ES and 1.6 ± 1 mm and 0.9 ± 0.3 mm for CF. CT scans from 153 patients were reviewed. ES and CF were identified in, respectively, 80% and 91% of cases, with a mean length and width of, respectively, 3.9 ± 0.8 mm and 0.8 ± 0.2 mm for ES.

Conclusion Large-sized ES was found frequently, and were clearly visible in patients CT scans. CF was markedly smaller, but seen in most patient scans. ES and CF could be areas of least resistance in the anterior part of the cribriform plate. CT might be helpful in understanding their pathological implications.

Keywords Cribriform plate · Ethmoid bone · Computed tomography · Skull base · Anatomy

Electronic supplementary material The online version of this article (https://doi.org/10.1007/s00276-019-02220-z) contains supplementary material, which is available to authorized users.

✉ Clément Escalard
clement.escalard@gmail.com

Lise-Marie Roussel
lisemarie61@yahoo.fr

Michèle Hamon
michele.hamon@unicaen.fr

Vincent Patron
patron-v@chu-caen.fr

Martin Hitier
hitier-m@chu-caen.fr

1 Department of Radiology, Centre Hospitalier Universitaire de Caen, 14000 Caen, France

2 Department of Otorhinolaryngology, Centre Hospitalier Universitaire de Caen, 14000 Caen, France

3 Department of Radiology, Centre Hospitalier Universitaire de Lille, 59000 Lille, France

4 Department of Anatomy, UNICAEN, 14032 Caen, France

5 INSERM U 1075 COMETE, 14032 Caen, France

Abbreviations

CF	Cribroethmoidal foramen
CSF	Cerebrospinal fluid
CT	Computed tomography
ES	Ethmoidal slit
HU	Hounsfield units
ICC	Intraclass correlation coefficient
IOM	Infraorbitomeatal
OM	Orbitomeatal
SOM	Supraorbitomeatal

Introduction

Recent progress in endoscopic surgery and radiology have made possible better understanding of the pathological processes involving the olfactory cleft and cribriform plate of the ethmoid. Several studies demonstrated that most cerebrospinal fluid (CSF) rhinorrhea occurred at the cribriform plate, renewing interest in this anatomical area [21–23].

The cribriform plate has many openings: the olfactory foramina, and two other pairs of openings in its anterior

part, which were described more than a century ago but have been largely ignored since [12, 19]. The ethmoidal slit (ES) is a long opening next to the Crista Galli, described by Gray [10], occupied by a process of dura mater. Also named "ethmoidal foramen", we will use the term "ethmoidal slit", to avoid any confusion with the anterior ethmoidal foramen: the internal opening of the anterior ethmoidal canal into the olfactory fossa (see anatomical scheme, Fig. 1).

The cribroethmoidal foramen (CF) is a smaller, round opening, anterior and lateral to the ES, which contains the anterior nasal artery (branch of the anterior ethmoidal artery), and the anterior ethmoidal nerve [9, 17]. Hooper described the cribriform plate's foramina on dry skulls, and revealed significant frequency and size of ES, with a mean length of 5.2 mm [12]. He hypothesized that it was the most common site for spontaneous CSF rhinorrhea because of abnormal bony defects, also because of its physiological openings, especially ES [12]. This was then emphasized by Patron et al. [19], who were also surprised by the few studies on the foramina of the cribriform plate. They studied the anterior part of the cribriform plate after anatomical dissections of four cadaver heads. ES and CF were found in four and three cases, respectively [19]. To our knowledge, no other study than Hooper et al. and Patron et al. described the anatomy of ES and CF.

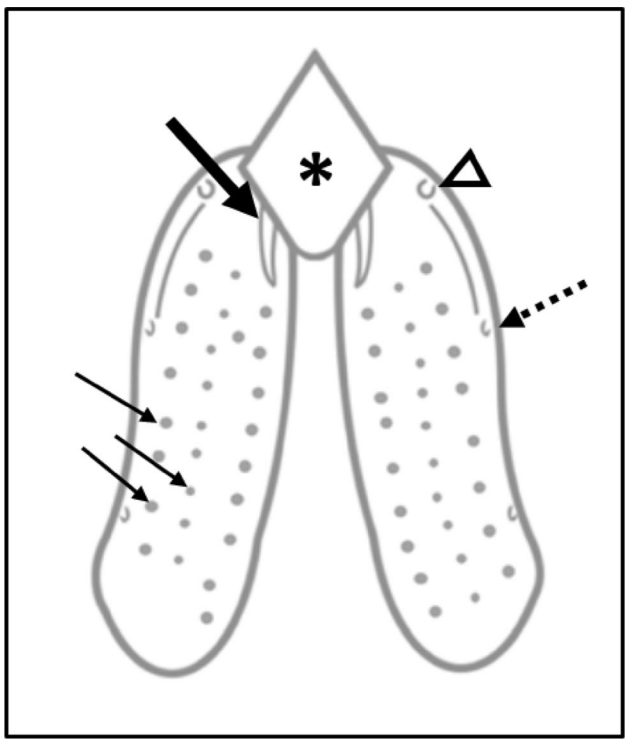

Fig. 1 Superior endocranial scheme of the cribriform plate and its main foramina. Thick arrow: ethmoidal slit (anterior part hidden by the Crista Galli), empty arrowhead: cribroethmoidal foramen, dashed arrow: anterior ethmoidal foramen, thin arrows: olfactory foramina, Crista Galli: star

As neither of these studies contains any radiological description of these foramina, it is still not known if they are visible with imaging. Because these foramina can be areas of weakness in the anterior cribriform plate, they possibly promote spontaneous CSF leaks, meningoceles, the spread of tumors, and increase susceptibility to traumatic injuries. Consequently, clinicians need imaging techniques to explore them on patients.

The aims of this study were to determine whether ES and CF are visible with conventional computed tomography (CT), and to record their frequency, dimensions and anatomical variants.

Methods

We conducted a two-part anatomical and radiological study: first on dry skulls, then on patient CT scans.

Anatomical and radiological study on dry skulls

Dry macerated skulls from voluntary body donators were provided by the University's Anatomy Department. Each piece was inspected for post-mortem damages. If the anterior part of one side of the cribriform plate was damaged, or if a foramen had irregular margins, it was excluded from ES and/or CF analysis. The presence, number, and anatomical variants of the ES and CF were determined by two observers. The longest length and width (anteroposterior diameter, and transverse diameter, respectively) of the ES and CF were measured using a surgical microscope (M320 F12, Leica Microsystems, Wetzlar, Germany) combined with a calibrated ocular micrometer, from the inferior aspect of the anterior skull base.

A CT study of the same skulls was then performed, using a 64-slice Optima CT660 conventional CT scanner (General Electric Healthcare, Boston, Massachusetts). Helicoidal acquisition parameters to explore adult petrous temporal bones from our institution were used, to obtain optimal spatial resolution (140 kV, 170 mA, slice thickness = 0.625 mm, matrix = 512 × 512 pixels, gantry rotation time = 1 s, collimation = 0.625 mm, field of view = 18 × 18 cm—modified in some cases according to patient dimensions). To reinforce the anatomical radiological correlation, 3/0 surgical ligature wires (Nichrominox, Saint Bonnet de Mure, France) were placed in the ES and CF, and used as landmarks [25] (see Online Resource 1). Each scan was examined in multiplanar reconstruction mode (window level = 200 Hounsfield Units (HU), window width = 3000 HU), using a McKesson Radiology Station (McKesson Radiology, San Francisco, California). The presence, number, and anatomical variants of the ES and

CF were determined. Their longest length and width were measured at their lowest parts. The length and width of the ES were measured using three different planes to determine which was the most appropriate for a radiological description of the ES: the orbitomeatal (OM), supraorbitomeatal (SOM), and infraorbitomeatal (IOM) planes (see Online Resource 1). The planes parallel to the OM, SOM and IOM were successively used during ES measurement phase. If an ES was entirely seen in one slice parallel to the plane concerned, this plane was considered useful for measuring ES, and the dimensions were finally recorded. If not, the plane concerned was considered inadequate because measuring the entire ES was not possible. CF was measured using planes perpendicular to their long axis.

Patients' CT scan study

We retrospectively reviewed all petrous bone CT scans performed between January 2012 and March 2016, with the same scanner, available in the Picture Archiving and Communication System of our institution. Exclusion criteria were part of the ethmoid bone or nasion outside of the field of view, movement artifacts, craniofacial or auricular malformation(s), previous ear surgery with removal of the whole scutum, previous trauma with displacement of the regions of interest (ES, CF, cribriform plate, scutum, nasion), olfactory cleft opacification, uncompleted Crista Galli or cribriform plate ossification. Acquisition parameters were the same as those used previously, except for children under the age of 12, for whom kV and mA were decreased. Each patient's CT was interpreted using multiplanar reconstructions. Orientation of the main reading plane was parallel to the most appropriate anatomical plane (OM, SOM or IOM, determined in the previous section). ES and CF were searched for. If they were present and considered sufficiently clear, their dimensions were recorded (main reading plane for ES, plane perpendicular to the long axes for the CF).

Statistical analysis

The intraclass correlation coefficient (ICC) between ES microscopic measurements and ES scan measurements (OM plane) was calculated. The correlation coefficient between the patients' age and ES sizes was calculated (Pearson coefficient). Differences in ES sizes according to gender or side were searched for (analysis of variance). p values of <0.05 were considered statistically significant. All calculations were made using IBM-SPSS software, V22.0 (IBM, Armonk, New York).

Ethics and patient consent

Written consents for research on anatomic specimens were obtained when the persons were still alive. Institutional Review Board approval was not required because research was performed on anatomic specimens and on a database.

Results

Anatomical and radiological study of dry skulls

Thirteen dry skulls (26 sides) were studied. Two sides were excluded from ES analysis and three sides were excluded from CF analysis because they were damaged.

ES was present in 92% of sides (22/24). Twenty ES looked like standard anatomical descriptions: one long narrow opening per side (Fig. 2). Two ES were partitioned, with a thin bony wall separating them into two parts, anterior and posterior. ES were not clearly identified in the remaining two sides. Using a surgical microscope, mean ES length was 4.3 ± 1.9 mm (range 2–8.6 mm), mean ES width was 1.3 ± 0.9 mm (range 0.2–1.6 mm) (see Online Resource 2).

All ES (22/22) were visible on CT (Fig. 3), and were measurable in 95% of cases (21/22) using the OM and SOM

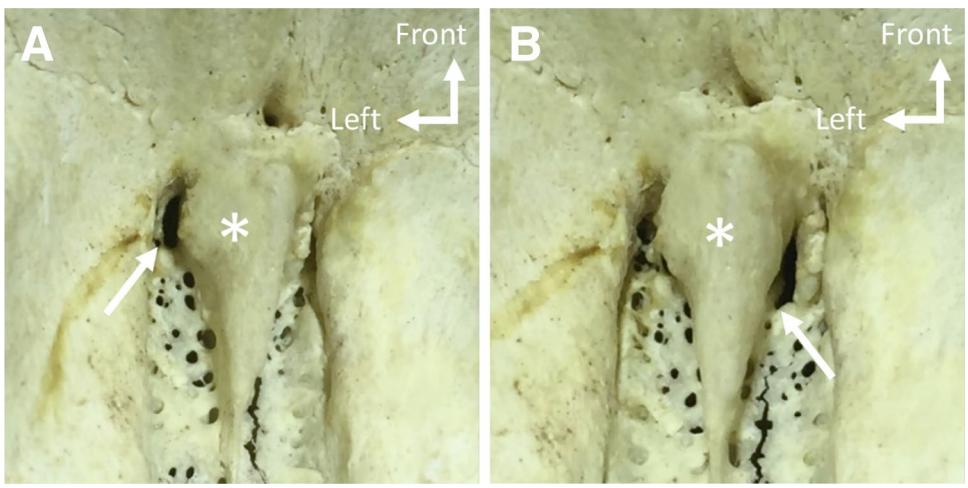

Fig. 2 Endocranial views of the cribriform plate in a dry skull (piece n°4): left superior oblique (**a**) and right superior oblique (**b**) views. Standard configuration of left (**a**) and right (**b**) ethmoidal slits (arrows), Crista Galli (stars)

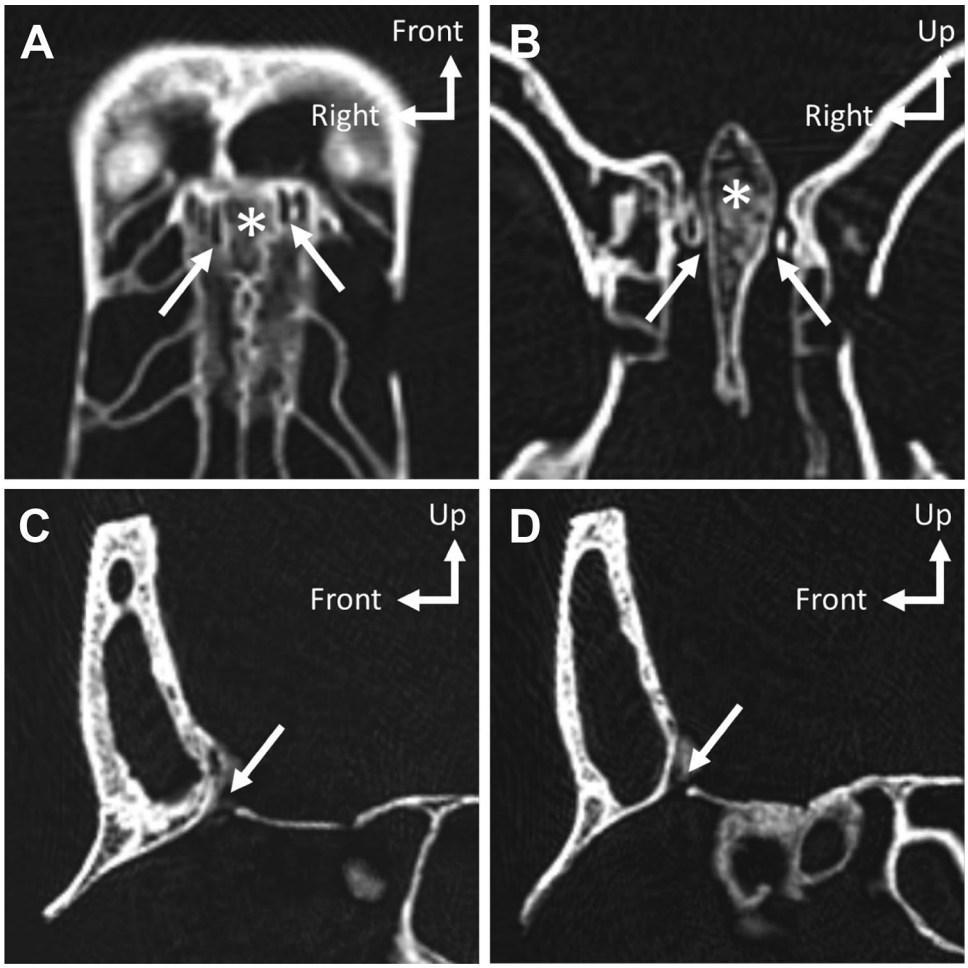

Fig. 3 CT scan of the cribriform plate in a dry skull (piece n°4): axial oblique, parallel to orbitomeatal plane (**a**), coronal (**b**), and sagittal—right side (**c**) and left side (**d**)—views. Standard configuration of ethmoidal slits (arrows): one long, narrow opening per side, behind the posterior wall of the frontal bone. Crista Galli (stars)

planes, and in 45% of cases (10/22) using the IOM plane (see Online Resource 3). As the OM plane was the best known plane, and made it possible to measure most of ES, it was chosen for the remaining study. Using CT, mean ES length was 3.9 ± 1.7 mm (range 1.2–7 mm) and mean ES width was 0.9 ± 0.3 mm (range 0.4–1.4 mm). ICC between surgical microscope and CT measurements (using OM plane) was excellent for lengths (ICC = 0.804 [0.577–0.915], $p < 0.001$) and poor for widths (ICC = 0.321 [0.000–0.655], $p = 0.073$).

CF was present in 100% of sides (23/23) (Fig. 4). Four CF looked like standard anatomical descriptions: one small, round opening per side. Nineteen CF were partitioned, with

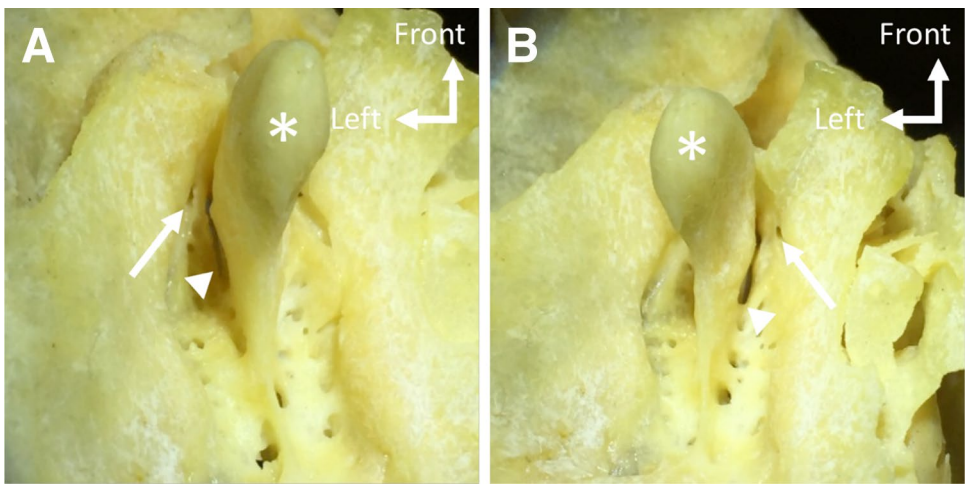

Fig. 4 Endocranial views of the cribriform plate in a dry skull (piece n°1): left superior oblique (**a**), right superior oblique (**b**) views. Standard configuration of cribroethmoidal foramina, one small, round opening per side: left (**a**) and right (**b**) cribroethmoidal foramina (arrows). Ethmoidal slits (arrowheads), Crista Galli (stars)

one or several thin bony septa. Using a surgical microscope, mean CF length was 1.5 ± 0.7 mm (range 1.1–3.1 mm), mean CF width was 0.8 ± 0.4 mm (range 0.2–1.3 mm) (see Online Resource 4).

All CF were visible on CT (23/23) (Fig. 5). Six were of standard appearance. Seventeen CF had different anatomical variants, particularly bony subdivisions into several smaller channels terminating at the olfactory cleft, frontal sinuses, frontal accessory cells (14/17). Two CF were partitioned. One CF was accompanied by an accessory canal, which was parallel to the lateral lamella. Using CT, mean CF length was 1.6 ± 1.1 mm (range 0.8–5.6 mm), mean CF width was 0.9 ± 0.3 mm (range 0.5–1.9 mm) (see Online Resource 5).

Patients' radiological study

CT scans of temporal petrous bones were performed on 257 patients. One hundred and four patients were excluded, mainly because of incomplete ethmoid bone exploration (68 cases) (see Online Resource 6). One hundred and fifty-three patients (306 sides) were, therefore, analyzed. Mean age was 38.7 ± 23.4 years (range 2–87 years). Sex ratio was 0.96.

ES was visible in 80% of sides (244/306) (Fig. 6). Of the 62 remaining sides, ES was replaced by several smaller foramina (20 sides), and a small gutter, without opening in the olfactory cleft (1 side). It was impossible for us to assess whether ES was present but too small to be seen, or really absent for the remaining 41 sides (lack of spatial resolution). When visible, ES was considered sufficiently clear to be measured in 74% of cases (181/244). Mean ES length and width were, respectively, 3.9 ± 0.8 mm (range 1–9 mm) and 0.8 ± 0.2 mm (range 0.4–1.7 mm). There were no significant differences between right and left sides (length $p = 0.38$, width $p = 0.48$). No correlation was found between these dimensions and patients' age, or between length and patients' sex. ES was slightly wider in men than in women (0.9 ± 0.2 mm versus 0.8 ± 0.2 mm, $p = 0.001$).

CF was visible in 91% of sides (278/306) (Fig. 6). In the remaining 28 sides, it was impossible for us to assess whether CF was present or not, due to lack of spatial resolution. Because of their small sizes and blurred contours, CF measurement was not possible.

Detailed data for each patient are available as Online Resource 7.

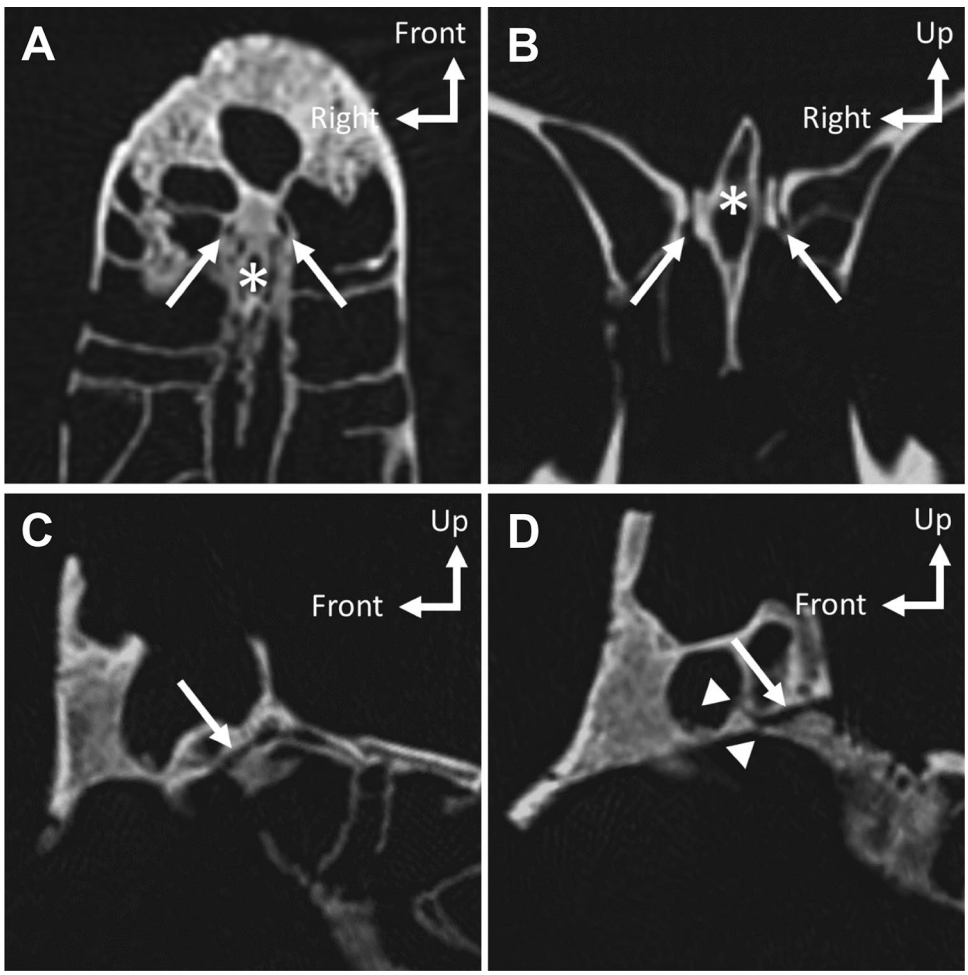

Fig. 5 CT scan of the cribriform plate in a dry skull (piece n°1): axial oblique parallel to the orbitomeatal plane (**a**), coronal (**b**), and sagittal—right side (**c**) and left side (**d**)—views. Cribroethmoidal foramina (arrows), with two subdivisions in the left one (arrowheads). Crista Galli (stars)

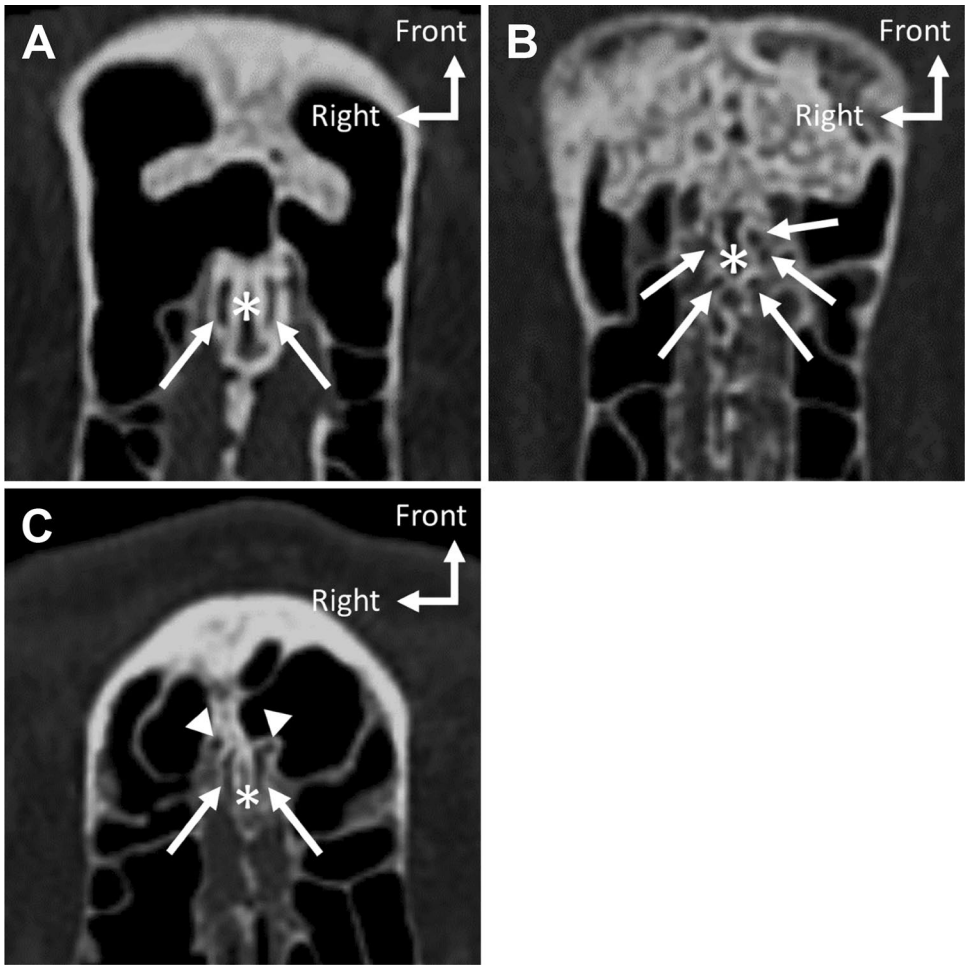

Fig. 6 CT scan of the cribriform plate in a patient: axial oblique—parallel to the orbitomeatal plane—view (**a**): standard configuration of ethmoidal slits (arrows). Example of anatomical variant in another patient: axial oblique—parallel to the orbitomeatal plane—view (**b**): ethmoidal slits replaced by several smaller foramina on both sides (arrows). CT scan of the cribriform plate in another patient: axial oblique view (**c**): both cribroethmoidal foramina are clearly visible (arrowheads). Ethmoidal slits (arrows). Crista Galli (stars)

Discussion

To our knowledge, this work is the first to study ES and CF using CT. It demonstrates that CT is able to identify these foramina, and gives an initial overview of their aspect, size, frequency, and anatomical variants. The OM plane is a valid plane for identifying and measuring ES using CT. ES was seen in 80% of sides in patients, with a mean length of 3.9 ± 0.8 mm, in agreement with previous studies [12, 19]. In some subjects, ES is much larger than bony defects responsible for CSF leaks [21], which underlines its potential pathological implication. CF was seen in 90% of sides in patients and had smaller dimensions.

Surprisingly, only few studies have been conducted on this topic, despite the pathological implications of the cribriform plate, and the past descriptions of ES and CF in anatomical textbooks. We only found three previous reports showing CT images of ES or CF. Neither studied these foramina. Gentry et al. [7] described the radiological anatomy of facial bones, ES was shown on a coronal CT section. Monjas-Cánovas et al. [18] conducted an angioscanographic study of the ethmoidal arteries. One of the coronal CT sections showed the terminal branch of the anterior ethmoidal artery passing through the cribriform plate, in what appeared to correspond to CF. Terrier et al. [24] described the normal CT anatomy of the ethmoid in two cadaver heads. CF can be seen in one of the coronal CT slices, referred as "ethmoidal split". Other anatomical studies of the anterior cranial base have already been performed, but many of them focused on paranasal sinus variations, especially on the height of the olfactory fossa [2, 11, 16]. Several studies described the cribriform plate's bone composition using CT [6], the cribriform plate's dimensions [3], the anatomical variations of the anterior ethmoidal artery [1], and new radiological signs of CSF leaks in the olfactory cleft [8, 13].

Our results highlight Hooper's findings and theory [12]. ES could explain the frequent involvement of the cribriform plate in CSF rhinorrhea: serving as a crossing point, or contributing to the formation of bony defects. They may be considered as additional points of least resistance at the anterior cranial base, like the lateral lamella of the ethmoid [14]. Assuming that ES and CF may facilitate certain diseases, the anterior part of the cribriform plate

should be carefully studied on CT scan and/or MRI in some pathological contexts, such as CSF rhinorrhea. Using the CT multiplanar reconstruction mode, the orbitomeatal plane and the coronal plane (perpendicular to it) make it easy to locate the Crista Galli, then to analyze the cribriform plate next to it, to search the ES on both sides of the inferior part of the Crista Galli, and the CF, anterior and lateral to the ES, along each lateral lamella of the ethmoid.

There were discrepancies between our results and those of the former studies, in terms of the dimensions and anatomical variants of ES [12, 19]. In Hooper's study, ES had a mean length of 5.2 mm, which is slightly higher than in our work, and were found in only 52% of cases. This could be explained by differences in the number of cases studied associated with sampling fluctuations, the methodology of the measurements (Hooper used Vernier calipers, and did not mention where the ES was precisely measured [12]), potential demographic variations, and subtleties in the terminology. What we designated as a "partitioned ES" was perhaps described by Hooper as "several large openings" [12]. We did not find any correlation between age and ES size. Appositional bone deposits may be responsible for the age-related decrease in the size of the olfactory foramina observed in one study [15], although this phenomenon may not involve ES. Some pathological processes could, conversely, widen intracranial foramina, as in idiopathic intracranial hypertension. The chronic increase in intracranial pressure may cause progressive thinning of bony walls and then herniations of the dura mater through it. This may occur preferentially in certain areas of weakness, such as the cribriform plate [20], especially at extravenous arachnoid granulations, which may instigate skull base erosion [4, 5]. ES and CF may act similarly and contribute to the formation of osteodural defects.

Our study has limitations. First, maceration was used to obtain dry skulls, exposing tiny parts such as cribriform plate to damages. Each piece was carefully checked to rule out any deterioration of ES and CF. Second, we used petrous bone CT for this study. The acquisition parameters of petrous bone CT had higher kV and mA than those commonly used to explore paranasal sinuses, to optimize the chances of viewing ES and CF. This choice also allowed to limit the risk of disease involving the cribriform plate, which may create acquired bony defects and modify its appearance. The current study should so be completed by analyzing paranasal sinuses CT to see if routine acquisition parameters can be used to examine ES and CF. We cannot recommend that the settings we used be maintained systematically, as this would increase irradiation and not comply with radiation protection guidelines. A case-by-case adaptation could, however, be made in certain pathological situations, if the acquisition parameters are found to be insufficient, and if the pathological involvement of ES and CF was to be demonstrated.

Conclusion

ES is a common structure, identified in 80% of sides in patient scans, with a mean length of 3.9 ± 0.8 mm. CF is also visible in 90% of sides in patient scans but too small to be precisely measured by imaging. These results provide new landmarks when interpreting facial CT scans. ES and CF need to be checked as possible areas of weakness in the anterior part of the cribriform plate, although their pathological involvement remains to be proved.

Author contributions CE: protocol development, data collection and management, data analysis, and manuscript writing. L-MR: protocol development and data collection. MH: protocol development and manuscript editing. AK: protocol development. VP: protocol development and manuscript editing. MH: protocol development and manuscript editing.

Compliance with ethical standards

Conflict of interest The authors declare that they have no conflict of interest.

References

1. Abdullah B, Lim EH, Husain S et al (2018) Anatomical variations of anterior ethmoidal artery and their significance in endoscopic sinus surgery: a systematic review. Surg Radiol Anat. https://doi.org/10.1007/s00276-018-2165-3
2. Adeel M, Ikram M, Rajput MSA et al (2013) Asymmetry of lateral lamella of the cribriform plate: a software-based analysis of coronal computed tomography and its clinical relevance in endoscopic sinus surgery. Surg Radiol Anat 35:843–847
3. Coelho DH, Pence TS, Abdel-Hamid M et al (2018) Cribriform plate width is highly variable within and between subjects. Auris Nasus Larynx 45:1000–1005
4. Connor SEJ (2010) Imaging of skull-base cephalocoeles and cerebrospinal fluid leaks. Clin Radiol 65:832–841
5. Gacek RR, Gacek MR, Tart R (1999) Adult spontaneous cerebrospinal fluid otorrhea: diagnosis and management. Am J Otol 20:770–776
6. Ganjaei KG, Soler SM, Mappus ED et al (2018) Novel radiographic assessment of the cribriform plate. Am J Rhinol Allergy 32:175–180
7. Gentry LR, Manor WF, Turski PA et al (1983) High-resolution CT analysis of facial struts in trauma: 1. Normal anatomy. Am J Roentgenol 140:523–532
8. Gharzouli I, Verillaud B, Tran H et al (2015) Value of systematic analysis of the olfactory cleft in case of cerebrospinal rhinorrhea: incidence of olfactory arachnoid dilatation. Eur Arch Otorhinolaryngol 18:1–5
9. Gleeson M (2008) Scott-Brown's otorhinolaryngology, head and neck surgery, vol 2, 7th edn. Hodder Arnold, London, p 1335
10. Gray H (1858) Anatomy: descriptive and surgical, 1st edn. John W Parker and Son, London, pp 55–56
11. Güldner C, Zimmermann AP, Diogo I et al (2012) Age-dependent differences of the anterior skull base. Int J Pediatr Otorhinolaryngol 76:822–828

12. Hooper ACB (1982) The cribriform plate and cerebrospinal fluid rhinorrhoea. Ir J Med Sci 151:31–35
13. Hoxworth JM, Glastonbury CM, Fischbein NJ et al (2008) Focal opacification of the olfactory recess on sinus CT: just an incidental finding? Am J Neuroradiol 29:895–897
14. Kainz J, Stammberger H (1989) The roof of the anterior ethmoid: a place of least resistance in the skull base. Am J Rhinol 3:191–199
15. Kalmey JK, Thewissen J, Dluzen DE (1998) Age-related size reduction of foramina in the cribriform plate. Anat Rec 251:326–329
16. Kaplanoglu H, Kaplanoglu V, Dilli A et al (2013) An analysis of the anatomic variations of the paranasal sinuses and ethmoid roof using computed tomography. Eurasian J Med 45:115–125
17. Lang J (1983) Clinical anatomy of the nose, nasal cavity and paranasal sinuses, 1st edn. Thieme, New York, p 128
18. Monjas-Cánovas I, García-Garrigós E, Arenas-Jiménez JJ et al (2011) Radiological anatomy of the ethmoidal arteries: CT cadaver study. Acta Otorrinolaringol Esp 62:367–374
19. Patron V, Berkaoui J, Jankowski R et al (2015) The forgotten foramina: a study of the anterior cribriform plate. Surg Radiol Anat 37:835–840
20. Schlosser RJ, Bolger WE (2004) Nasal cerebrospinal fluid leaks: critical review and surgical considerations. Laryngoscope 114:255–265
21. Schuknecht B, Simmen D, Briner HR et al (2008) Nontraumatic skull base defects with spontaneous CSF rhinorrhea and arachnoid herniation: imaging findings and correlation with endoscopic sinus surgery in 27 patients. Am J Neuroradiol 29:542–549
22. Shetty PG, Shroff MM, Sahani DV et al (1998) Evaluation of high-resolution CT and MR cisternography in the diagnosis of cerebrospinal fluid fistula. Am J Neuroradiol 19:633–639
23. Stone JA, Castillo M, Neelon B et al (1999) Evaluation of CSF leaks: high-resolution CT compared with contrast-enhanced CT and radionuclide cisternography. Am J Neuroradiol 20:706–712
24. Terrier F, Weber W, Ruefenacht D et al (1985) Anatomy of the ethmoid: CT, endoscopic, and macroscopic. Am J Roentgenol 144:493–500
25. Trost O, Kazemi A, Cheynel N et al (2009) Spatial relationships between lingual nerve and mandibular ramus: original study method, clinical and educational applications. Surg Radiol Anat 31:447–452